Toll-like receptor 2 activation and upregulation by high mobility group box l contribute to postoperative neuroinflammation and cognitive dysfunction in mice

Fei Lin[1,2], **Weiran Shan**[1], **Yuxin Zheng**[1,3], **Linghui Pan**[2], **Zhiyi Zuo**[1]

[1]Department of Anesthesiology, University of Virginia, Charlottesville, Virginia

[2]Department of Anesthesiology, Guangxi Medical University Cancer Hospital, Nanning, China

[3]Department of Anesthesiology, General Hospital of Tianjin Medical University, Tianjin, China

Abstract

Postoperative cognitive dysfunction (POCD) is common and is associated with poor clinical outcome. Toll-like receptor (TLR) 3 and 4 have been implied in the development of POCD. The role of TLR2, a major brain TLR, in POCD is not clear. High mobility group box-l (HMGBl) is a delayed inflammatory mediator and may play a role in POCD. The interaction between HMGB1 and TLRs in the perioperative period is not known. We hypothesize that TLR2 contributes to the development of POCD and that HMGB1 regulates TLR2 for this effect. To test these hypotheses, 6- to 8-week old male mice were subjected to right carotid artery exposure under isoflurane anesthesia. CU-CPT22, a TLR1/TLR2 inhibitor, at 3 mg/kg was injected intraperitoneally 30 min before surgery and one day after surgery. Glycyrrhizin, a HMGB1 antagonist, at 200 mg/kg was injected intraperitoneally 30 min before surgery. Mice were subjected to Barnes maze and fear conditioning tests from 1 week after surgery. Hippocampus and cerebral cortex were harvested 6 h or 12 h after the surgery for Western blotting, ELISA, immunofluorescent staining and chromatin immunoprecipitation. There were neuroinflammation and impairment of learning and memory in mice with surgery. Surgery increased the expression of TLR2 and TLR4 but not TLR9 in the brain of CD-1 male mice. CU-CPT22 attenuated surgery-induced neuroinflammation and cognitive impairment. Similarly, surgery induced neuroinflammation and cognitive dysfunction in C57BL/6J mice but not in TLR2$^{-/-}$ mice. TLR2 staining appeared in neurons and microglia. Surgery increased HMGBl in the cell nuclei of the cerebral cortex and hippocampus. Glycyrrhizin ameliorated this increase and the increase of TLR2 in the hippocampus after surgery. Surgery also increased the amount of *tlr2* DNA precipitated by an anti-HMGB1 antibody in the hippocampus. Our results suggest that TLR2 contributes to surgery-induced neuroinflammation and cognitive

impairment. HMGB1 upregulates TLR2 expression in the hippocampus after surgery to facilitate this contribution. Thus, TLR2 and HMGB1 are potential targets for reducing postoperative cognitive dysfunction.

Keywords

High mobility group box-l; neuroinflammation; postoperative cognitive dysfunction; toll-like receptors 2

1. Introduction

Postoperative cognitive dysfunction (POCD) is common in patients after anesthesia and surgery (Bedford, 1955; Monk et al., 2008; Terrando et al., 2011) and is associated with poor outcome, such as increased postoperative morbidity, mortality, hospital stay and cost of care (Moller et al., 1998; Steinmetz et al., 2009). The pathogenesis of POCD is not fully identified and clinically practical methods to reduce POCD have not been developed. These knowledge and methods are needed to reduce the occurrence of POCD.

Neuroinflammation may lead to cognitive impairment (d'Avila et al., 2018; McKim et al., 2016). We and others have shown that neuroinflammation may play a major role in POCD in animal models (Bi et al., 2017; Cao et al., 2012; Cibelli et al., 2010; Zhang et al., 2014a; Zhang et al., 2014b).

Toll-like receptors (TLRs) are a conserved family of pattern recognition receptors and play a central role in innate immunity and sterile inflammation (Kawai et al., 2010; Lin et al., 2011; Miyake, 2007). TLRs transmit extracellular signals to activate transcription factors, such as nuclear factor-κB, which results in production of proinflammatory cytokines (Lin et al., 2011; Miyake, 2007). Among the 13 types of TLRs, TLR2 and TLR4 are the major ones that can bind components of cells and tissues (Kawai et al., 2010). TLR4 has been shown to contribute to the neuroinflammation and cognitive dysfunction after surgery (Lu et al., 2015a; Wang et al., 2013). A recent study showed that extracellular RNAs-TLR3 played a role in learning and memory dysfunction after nephrectomy in mice (Chen et al., 2019) . We have shown that TLR2 may be a mediator for sepsis-induced encephalopathy in mice (Xing et al., 2018). Although there are overlapping pathological processes and presentations, such as inflammation and cognitive impairment, between sepsis-induced encephalopathy and POCD, significant differences exist between these two conditions. For example, sepsis often involves pathogens but surgery is performed under sterile conditions. Previous studies have shown that surgery increases TLR2 in rats (Feng et al., 2017; Muscat et al., 2021; Yang et al., 2020). However, the role of TLR2, a major brain TLR, in POCD is not known because these previous studies have not determined whether the increased TLR2 is an associated phenomenon with POCD or contributes to POCD.

High mobility group box-l (HMGBl) is found in mammalian cell nuclei (Lotze et al., 2005) and supports transcription of genes (Klune et al., 2008). Extracellular HMGB1 can act as a damage signaling molecule to promote the movement of immune cells towards the lesion site and activate the inflammatory reaction (Faraco et al., 2007; Festoff et al., 2016; Scaffidi

et al., 2002). One of the possible mechanisms is that HMGB1 can bind and activate TLR2 and TLR4 (Aucott et al., 2018; Bae, 2012; Park et al., 2004; Yu et al., 2006) . The role of HMGB1 in POCD has been implied (Terrando et al., 2016; Vacas et al., 2014). However, the interaction between HMGB1 and TLRs after surgery is not known. The mechanisms for surgery to affect the expression of TLRs have not been reported.

Thus, we hypothesize that TLR2 contributes to surgery-induced neuroinflammation and the impairment of learning and memory and that HMGB1 regulates TLR2 expression for these effects. To test these hypotheses, mice with or without TLR2 knockout were subjected to surgery and anesthesia. Their learning and memory were tested.

2. Materials and Methods

The institutional Animal Care and Use Committee of the University of Virginia (Charlottesville, VA, USA) had approved our animal protocol (#3114). The animal studies were performed in compliance with the National Institutes of Health Guide for the Care and Use of Laboratory Animals (NIH publications number 80–23) revised in 2011.

This study did not involve human subjects and was not pre-registered.

2.1. Animal groups

Six- to eight-week old male CD-1 mice weighing 28 - 32 g from Charles River Laboratories International Inc. (RRID:IMSR_CRL:022) were arbitrarily assigned to: (1) control group (not being exposed to surgery or any medications) and (2) surgery group (right carotid artery exposure) in the first experiment. In the second experiment, the mice were assigned to: (1) control group, (2) surgery group, (3) CU-CPT22 group, (4) surgery plus CU-CPT22 group and (5) surgery plus dimethyl sulfoxide (DMSO) group. CU-CPT22 was used as a TLR1/TLR2 inhibitor (Cheng et al., 2012). DMSO was a solvent for CUCPT22. In the third experiment, 6- to 8-week old male TLR2 knockout mice (TLR2$^{-/-}$ mice, The Jackson Laboratory, RRID:IMSR_JAX:004650) and their wild-type controls (C57BL/6J mice, The Jackson Laboratory, RRID:IMSR_JAX:000664) were used in this study. These mice were arbitrarily assigned to: (1) TLR2$^{-/-}$ mouse control group, (2) TLR2$^{-/-}$ mouse surgery group, (3) wild-type C57BL/6J mouse control group and (4) wild-type C57BL/6J mouse surgery group. In the fourth experiment, CD-1 mice were arbitrarily assigned to: (1) control group, (2) glycyrrhizin group, (3) surgery group and (4) surgery plus glycyrrhizin group. Glycyrrhizin was used as a HMGB1 antagonist (Kong et al., 2017) . The mice were housed in standard mouse cages (27.94×15.24×11.43 cm) with 3 to 5 mice in each cage and with *ad libitum* access to food and water. The cages were kept in a quiet, 12-h light/dark cycle standard environment. In total, 219 mice were used in this study. There were no predetermined criteria to exclude animals once they were assigned to a study group.

Three separate cohorts of mice were used for experiments. One cohort (15 mice per group for experiment 2 and 7 mice per group for experiment 3) was used for learning and memory tests that were started from one week after the surgery. Second cohort was used for harvesting brain tissues at 6 h after surgery for Western blotting (6 or 10 mice per group), immunofluorescent staining (4 mice per group) and chromatin immunoprecipitation

(15 mice per group). The third cohort was used for harvesting bilateral cerebral cortex and hippocampus at 12 h after surgery for ELISA (6 mice per group). The time-line of experimental procedures was as shown in figure 1.

2.2. CU-CPT22 and glycyrrhizin application

CU-CPT22 (Millipore, catalogue number 614305) was dissolved in DMSO and injected intraperitoneally at 3 mg/kg 30 min before surgery and one day after surgery. The CU-CPT22 dose was chosen based on previous studies (Cheng et al., 2012; Ji et al., 2015). Acetic acid was used to dissolve glycyrrhizin acid ammonium salt (Santa Cruz, catalogue number sc-203059) that was intraperitoneally injected at 200 mg/kg 30 min before surgery. This dose was selected based on a previous study (Kim et al., 2015).

2.3. Anesthesia and surgery

The surgery was a right carotid artery exposure. Mice were anesthetized by 1.8% isoflurane, which was commonly used for mice to have surgery as we described before (Zeng et al., 2021; Zhang et al., 2014b; Zheng et al., 2017). During the procedure, the mouse was kept at spontaneous respiration and rectal temperature was monitored and maintained at 37°C with the aid of a heating blanket (TCAT-2LV, Physitemp Instruments Inc., Clifton, NJ). A 1.5-cm midline neck incision was made after the mouse was exposed to isoflurane for at least 30 min. Soft tissues covering the trachea were dissected bluntly. One centimeter long right common carotid artery was carefully dissected free from adjacent tissues without any damage on vagus nerve. The wound was then irrigated and closed by using surgical suture. The surgical procedure was performed under sterile conditions and lasted around 10 min. As shown in our previous study, mice having this surgery under isoflurane anesthesia did not have hypoxia and had heart rates and respiratory rates within the normal ranges (Li et al., 2013). To reduce the pain after surgery, a subcutaneous injection of 3 mg/kg bupivacaine to the incision site was given to all animals. The anesthesia duration was 2 h. The anesthesia level was maintained at no response to toe pinching and surgery. These measures were used to reduce/prevent suffering of mice during and after the surgery.

2.4. Barnes maze

As shown in figure 1, mice were subjected to Barnes maze one week after various experimental conditions for testing their spatial learning and memory as previously described (Cao et al., 2012; Zhang et al., 2014b; Zheng et al., 2017). The test was performed between 1:00 to 6:00 pm. The Barnes maze circular platform has 20 holes that are equally spaced (SD Instruments, San Diego, CA, USA). One of the holes was connected to a dark chamber that was called target box. The test was started by placing animals in the middle of the platform. Aversive noise (85 db) and bright light from a 200-W bulb shed on platform were used to provoke mice to find and enter the target box. Animals were trained in a spatial acquisition phase that took 4 days with 3 min per trial, four trials per day and 15-min interval between each trial. The test was performed on day 5 (short-term retention) and day 12 (long-term retention) to evaluate the memory of the animals. There was no test between day 5 to day 12. An ANY-Maze video tracking system (SD Instruments) was used to calculate the latency to enter the target box during each trial.

2.5. Fear conditioning

The fear conditioning test was performed between 1:00 to 6:00 pm 24 h after the Barnes maze test in a way similar to that previously described (Cao et al., 2012; Zhang et al., 2014b; Zheng et al., 2017). Mice were placed in a test chamber wiped with 70% alcohol. They were subjected to three tone-foot shock pairings (tone at 2000 Hz and 85 db for 30 s; foot shock at 0.7 mA for 2 s) with 1-min interval between trials in a relatively dark room. Mice were removed from the test chamber 30 s after training and returned to their regular cages. Mice were placed 24 h later to the same chamber for 8 min without tone and shock. The freezing behavior was recorded in an 8-s interval (context-related learning and memory). Two hours later, mice were placed in a novel test chamber that had a different context and smell from the first test chamber. This chamber was wiped with 1% acetic acid and was in a relatively light room. After no stimuli for 3 min, the tone was played for three cycles with each cycle for 30 s followed by 1-min interval between cycles (total 4.5 min). Freezing behavior during the 4.5 min was recorded. The test was recorded by a camera and the video was scored for animal freezing behavior in the 4.5 min (tone-related learning and memory) by an observer who was blind to group assignment of animals.

2.6. Brain tissue harvesting

Mice were deeply anesthetized with isoflurane at 6 or 12 h after the surgery. They were perfused with normal saline (0.9% sodium chloride). The bilateral cerebral cortex and hippocampus were dissected for Western blotting of TLR2, TLR4, TLR9 and HMGB1 at 6 h after the surgery and ELISA of interleukin (IL)-1β or IL-6 at 12 h after the surgery. A coronal brain slice between Bregma −2 and −4 mm was harvested 6 h after the surgery for immunofluorescent staining. These slices containing hippocampus were fixed with 4% paraformaldehyde. The procedures for dissecting the brain were performed on ice.

2.7. Western blotting analysis

The cerebral cortex and hippocampus were homogenized in RIPA buffer (Thermo Scientific, catalogue number 89900) containing protease inhibitor cocktail (Sigma, cat# P2714) and phosphatase inhibitor cocktail (Roche Applied Science, catalogue number 04906845001). The solutions were centrifuged at 13,000 rpm at 4°C for 20 min. The resultant supernatant was kept as the total proteins. The homogenates were centrifuged at 4200 rpm for 10 min at 4°C and the supernatant was centrifuged at 33,300 rpm for 1 h at 4°C. The resultant pellet was re-suspended in lysis buffer and was homogenized with an ultrasound homogenizer on ice. The homogenates were saved as containing membrane proteins. The cytoplasmic and nuclear proteins were extracted by NE-PER nuclear and cytoplasmic extraction reagents (Pierce Biotechnology, catalogue number 78833) according to the manufacturer's instructions. The protein concentration was determined by a Pierce BCA protein assay kit (Pierce Biotechnology, catalogue number 23227).

Proteins of 20 μg per lane were separated on 12% polyacrylamide gels and then transferred onto a polyvinylidene difluoride membrane. The membranes were incubated with the following primary antibodies overnight at 4°C: rabbit monoclonal anti-TLR2 antibody (1:1000, Abcam, RRID: AB_10861644), rabbit polyclonal anti-TLR4 antibody (1:1000, Abcam, RRID: AB_10561435), mouse monoclonal anti-TLR9 antibody (1:1000,

Abcam, RRID: AB_298862), rabbit polyclonal anti-HMGB1 antibody (1:1000, Abcam, RRID: AB_444360), mouse monoclonal anti-β-actin antibody (1:5000, Abcam, RRID: AB_2223210) or rabbit polyclonal anti-lamin A antibody (1:1000, Abcam, RRID: AB_775965). Protein bands were visualized using a genomic and proteomic gel documentation systems (Gel Doc) from Syngene (Frederick, MD). The protein band intensities of TLR2, TLR4 and TLR9 from total and membrane proteins and HMGB1 from cytoplasmic proteins were normalized to those of β-actin. The results of HMGB1 from nuclear proteins were normalized to those of lamin A. The data of various experimental conditions were then normalized by the mean results of their control animals.

2.8. Quantification of IL-1β and IL-6

As we previously described (Lin et al., 2020), brain tissues were homogenized on ice in 20 mM Tris–HCl buffer (pH: 7.3) containing protease inhibitors (10 mg/ml aprotinin, 5 mg/ml pepstatin, 5 mg/ml leupeptin, and 1 mM phenylmethanesulfonylfluoride). The solutions were centrifuged at 13,000 rpm for 20 min at 4°C. The supernatant was saved and Bradford protein assay of the supernatant was performed for each sample. ELISA kits for measuring mouse IL-1β and IL-6 (R&D Systems, catalogue number MLB00C and M6000B) were used to quantify the contents of these cytokines in the samples according to the manufacturer's instructions. The quantity of IL-1β and IL-6 in each brain sample was standardized to the protein contents.

2.9. Immunohistochemistry

Similar to what we described previously (Zhang et al., 2014b; Zheng et al., 2017), brains were post-fixed at 4°C for 18 h in 4% paraformaldehyde in 0.1 M phosphate buffered saline, dehydrated, and embedded in paraffin. Coronal 5-μm sections of the cerebral hemisphere were cut sequentially and mounted on super-frost plus microscope slides. Antigen retrieval with Tris/EDTA buffer (10 mM Tris Base, 1 mM EDTA, 0.05% Tween 20, pH 9.0) was performed at 95 to 100°C for 20 min. After being washed in Tris-buffered saline (TBS) containing 0.025% triton-X 100, sections were blocked in 10% donkey serum plus 1% bovine serum albumin in TBS for 2 h at room temperature and then incubated at 4°C overnight with the following primary antibodies: rabbit polyclonalanti-TLR2 antibody (1:200, Thermo Scientific, RRID: AB_1087895), mouse monoclonal anti-glial fibrillary acidic protein (GFAP) antibody (1:200, Millipore, RRID: AB_11212597), goat polyclonal anti-ionized calcium binding adapter molecule 1 (Iba-1) antibody (1:1000, Abcam, RRID: AB_10972670) or mouse monoclonal anti-neuronal nuclei (NeuN) antibody (1:100, Millipore, RRID: AB_2298772). Sections were rinsed in TBS with 0.025% triton-X 100. The donkey anti-goat IgG antibody conjugated with Alexa Fluor 488 (1:200, Invitrogen, RRID: AB_2534102), donkey anti-rabbit IgG antibody conjugated with Alexa Fluor 488 (1:200, Invitrogen, RRID: AB_2535792), donkey anti-mouse IgG antibody conjugated with Alexa Fluor 594 (1:200, Invitrogen, RRID: AB_141633) or donkey anti-rabbit IgG antibody conjugated with Alexa Fluor 594 (1:200, Invitrogen, RRID: AB_141637) were incubated with the sections for 1 h at room temperature in the dark. After washed in TBS, sections were mounted and cover-slipped with Vectashield mounting medium (Vector Laboratories, catalogue number H-1000). A fluorescence microscope with a charge-coupled device camera was used to acquire immunostaining images.

2.10. Chromatin immunoprecipitation assay

The chromatin immunoprecipitation assay was conducted by using a Magna ChIP G-chromatin immunoprecipitation kit (Millipore, catalogue number 17-611) as we described before (Feng et al., 2014). Briefly, the hippocampus tissue was cross-linked by 1.5% formaldehyde for 15 min at room temperature. The cross-linking was stopped by glycine and the tissue was washed twice with cold phosphate buffered saline. The cross-linked tissue was grinded, followed by processing with a 28-gauge needle to get homogeneous suspension. The homogenate was subsequently lysed by the cell lysis buffer and nucleus lysis buffer supplied in the kit. About 200 - 500 base pair cross-linked DNA fragments were obtained by sonication. The resulting DNA fragments were incubated with a rabbit polyclonal anti-HMGB1 antibody (Abcam, RRID: AB_444360) or normal rabbit IgG (Millipore, RRID: AB_490574) at 1 μg/450 μl sample overnight, respectively. The immunoprecipitated DNA was used to detect the quantity of a fragment of *tlr2* promotor (−283 bp to −71 bp) by PCR assay. The primers were as follows: sense primer: 5'-CATAAGTAGGCAGTTTTGGTCAAGG-3'; anti-sense primer: 5'-GCAAGGATTCTGGAAGGAAGAGGAT-3'.

2.11. Blinding

The blinding practice was observed during the assessment of fear condition behavior. The video was evaluated by a person who did not perform the test and did not know the group assignment of animals. No blinding procedure was used for other experiments.

2.12. Statistical analysis

We did not perform sample size calculation for each experiment. The sample size was larger in experiments testing learning and memory than that in biochemical experiments, which was based on our experience (Bi et al., 2017; Zheng et al., 2017). Regardless, the minimal sample size for any groups or experimental conditions was 6. Parametric results in normal distribution in line plots are presented as mean ± S.E.M. (n ≥ 6). All other data are presented in box plots (n ≥ 6). The n number referred to the number of animals. The Kolmogorov-Smirnov test for normality was performed to assess whether the data was normally distributed. No test for outliers was performed. All data was included in the analyses. The data from the training sessions of Barnes maze test within the same group were tested by one-way repeated measures analysis of variance followed by Tukey test. Two-way repeated measures analysis of variance followed by Tukey test was used to analyze the data of the training sessions in Barnes maze test between groups. All other data were analyzed by t-test or one-way analysis of variance followed by the Tukey test if the data were normally distributed or by rank sum test or one-way analysis of variance on ranks followed by the Tukey test if the data were not normally distributed. The set of non-normally distributed data was identified in the figure legends. Differences were considered significant at $P < 0.05$ based on two-tailed hypothesis testing. All statistical analyses were performed with Sigma Stat 3.5 (Systat Software, Point Richmond, CA).

3. Results

No animal died during the experiments. Since no predetermined criteria were formed, data of all animals were included, analyzed and reported here.

3.1. TLR2 inhibition or knockout attenuated surgery-induced neuroinflammation and dysfunction of learning and memory

Compared with control group, the total TLR2 and TLR4 protein and their membrane fraction in the cerebral cortex and hippocampus of CD-1 mice with surgery were significantly increased. However, the total TLR9 protein and its membrane fraction in the cerebral cortex and hippocampus of mice with surgery were not affected (Figure 2). These results suggest that surgery induces differential expression of TLRs. Since the role of TLR4 in POCD has been implied (Lu et al., 2015a; Wang et al., 2013) and TLR2 is abundantly expressed in the brain (Xing et al., 2018) , we focused our investigation on TLR2. Immunofluorescent staining showed that TLR2 staining was co-localized with the staining of NeuN, a neuronal marker, and Iba-1, a microglial marker, but was not co-localized with the staining of GFAP, an astrocytic marker (Zhang et al., 2014b; Zheng et al., 2017) (Figure 3). These results suggest that TLR2 is expressed in the neurons and microglia but may not be expressed in the astrocytes.

The time for CD-1 mice to identify the target box was decreased with increased training sessions of Barnes maze test (Figure 4a). Surgery and anesthesia were not a significant factor to influence the time needed for mice to identify the target box during the training sessions [F(1,28) = 0.011, P = 0.917]. Similarly, CU-CPT22, a specific TLR2 antagonist (Cheng et al., 2012; Ji et al., 2015; Xing et al., 2018), was not a factor to affect this time in mice without surgery [F(1,28) = 3.430, P = 0.075]. However, surgery increased the time for mice to identify the target box 8 days after the training sessions. This surgery effect was attenuated by CU-CPT22 but not by DMSO, a solvent for CU-CPT22. CU-CPT22 did not affect the non-surgery mice to identify the target box 8 days after the training sessions (Figure 4b). Similar to the Barnes maze test results, context-related freezing behavior in the surgery group and surgery plus DMSO group was less than that of control group in the fear conditioning test. This reduction did not exist in the surgery plus CU-CPT22 group. CU-CPT22 did not affect the context-related freezing behavior of non-surgery mice (Figure 4c). These results suggest that anesthesia and surgery induces the dysfunction of long-term spatial memory and hippocampus-dependent cognition and that CU-CPT22 attenuates this dysfunction, indicating a role of TLR2 in the effect.

Compared with control group, the expression of IL-1β and IL-6 in the hippocampus and IL-6 in the cerebral cortex of CD-1 mice was increased in surgery group. This effect was ameliorated by CU-CPT22 (Figure 5a, b). These results suggest that surgery increases proinflammatory cytokines possibly via TLR2.

In order to further determine the role of TLR2 in surgery-induced neuroinflammatory responses and dysfunction of learning and memory, TLR2$^{-/-}$ mice were used. C57BL/6J mice are recommended by Jackson Laboratory as the control mice for TLR2$^{-/-}$ mice. Similar to the results of CD-1 mice, surgery increased IL-1β and IL-6 in the hippocampus

and cerebral cortex of C57BL/6J mice but did not alter the levels of IL-1β and IL-6 in the hippocampus and cerebral cortex of TLR2$^{-/-}$ mice (Figure 5c, d). The time for C57BL/6J and TLR2$^{-/-}$ mice to identify the target box was decreased with increased training sessions of Barnes maze tests (Figure 6a). Surgery and anesthesia were not a significant factor to influence the time needed for C57BL/6J or TLR2$^{-/-}$ mice to identify the target box during the training sessions [$F(1,12) = 0.501$, $P = 0.493$ for C57BL/6J mice, $F(1,12) = 0.148$, $P = 0.707$ for TLR2$^{-/-}$ mice]. Surgery increased the time needed for C57BL/6J mice to identify the target box one day and eight days after the training sessions (Figure 6b). Surgery also decreased the freezing behavior of C57BL/6J mice in the context-related fear conditioning tests. These surgery effects on the performance of C57BL/6J mice in the Barnes maze and fear conditioning tests did not appear in TLR2$^{-/-}$ mice (Figure 6c). These results support an important role of TLR2 in surgery-induced responses and dysfunction of learning and memory.

3.2. Surgery increased HMGB1 to increase TLR2 expression

As a first step to determine the role of HMGB1 in the surgery, the expression of HMGB1 was measured. Surgery increased the amount of HMGB1 in the nuclear fraction of the cerebral cortex and hippocampus of CD-1 mice but did not alter the amount of HMGB1 in the cytoplasmic fraction (Figure 7a, b). Glycyrrhizin, a HMGB1 antagonist (Kim et al., 2015; Kong et al., 2017), inhibited the increase of HMGB1 in the nuclear fraction of the cerebral cortex and hippocampus of CD-1 mice with surgery (Figure 7c–f). Glycyrrhizin also attenuated surgery-induced increase of total TLR2 protein in the cerebral cortex and hippocampus and its membrane fraction in the hippocampus (Figure 8a, c). These results suggest that HMGB1 may regulate the expression of TLR2 after surgery. Interestingly, the immunoprecipitate prepared by an anti-HMGB1 antibody contained an increased amount of *tlr2* DNA in mice with surgery (Figure 8d), indicating that HMGB1 may bind to *tlr2* DNA and that surgery increases this binding. These results suggest that HMGB1 regulates the expression of TLR2 after surgery. PCR was performed on four segments of presumed promoter region of *tlr2* with the immunoprecipitate prepared by the anti-HMGB1 antibody. Interestingly, only the fragment of −283 to −72 bp among the 2000 bp upstream of the transcription portion of the gene *tlr2* was amplified. The sequence of the fragment and the presumed HMGB1 binding sequence are presented in figure 8f.

4.   Discussion

Consistent with our previous studies (Cao et al., 2012; Zhang et al., 2014a; Zhang et al., 2014b; Zheng et al., 2017), our current study showed that surgery increases proinflammatory cytokines and induces learning and memory dysfunction in wild-type CD-1 mice, an outbred type of mice, and wild-type C57BL/6J mice, an inbred type of mice. We and others have shown that neuroinflammation is a critical neuropathological process for POCD (Cao et al., 2012; Zhang et al., 2014a; Zhang et al., 2014b; Zheng et al., 2017). However, the mechanisms for the occurrence of neuroinflammation are not fully defined.

TLRs are receptors that are involved in inflammatory responses (Kawai et al., 2010; Lin et al., 2011; Miyake, 2007). Each of the 13 TLRs has preferred ligands (Kawai et al., 2006).

For example, TLR2 and TLR4 bind cellular components of host, TLR3 binds RNAs and TLR9 interacts with components of pathogens (Kawai et al., 2006; Lin et al., 2011; Miyake, 2007). The role of TLR3 and TLR4 in POCD has been implied in previous studies (Chen et al., 2019; Lu et al., 2015a; Lu et al., 2015b; Wang et al., 2013). A recent study showed that cardiopulmonary bypass surgery increased TLR2 and TLR4 expression in the hippocampus of rats. An agonist of TLR2/TLR4 attenuated the protection of exosomes of stem cells on learning and memory in these rats (Yang et al., 2020). Our current study showed that surgery increased TLR2 and TLR4. Since TLR9 responds to pathogens (Kawai and Akira, 2006) and our surgery is a sterile procedure, we used TLR9 as a control TLR protein. As expected, surgery did not affect the expression of TLR9, suggesting that the increase of TLR2 and TLR4 is a specific effect of surgery. Since TLR2 is a major TLR in the brain and form TLR complex with TLR1 or TLR6 to induce inflammatory cytokine production (Kawai et al., 2006; Xing et al., 2018), TLR2 may be involved in surgery-induced neuroinflammation and cognitive dysfunction.

CU-CPT22 is a cell permeable antagonist for TLR1/TLR2 (Cheng et al., 2012). Our results showed that CU-CPT22 blocked surgery-induced proinflammatory cytokine production and dysfunction of learning and memory. In addition, surgery did not induce proinflammatory cytokine production and dysfunction of learning and memory of TLR$^{-/-}$ mice. These results suggest a vital role of TLR2 in neuroinflammation and cognitive impairment caused by surgery. Previous studies have shown that TLRs are mainly expressed in the microglia and neurons in the brain (Kilic et al., 2008; Lehnardt et al., 2007; Xing et al., 2018; Ziegler et al., 2007). Consistent with this finding, TLR2 was mostly expressed in neurons and microglia under control or surgery conditions.

One novel and important finding of our study is that HMGB1 regulates TLR2 expression for POCD. Extracellular HMGB1 is considered as a critical mediator for delayed inflammatory response in sepsis (Wang et al., 2014; Wang et al., 2004). HMGB1 can activate the innate immune system following the aseptic trauma of surgery to result in postoperative neuroinflammation and cognitive impairment (Kong et al., 2017; Lin et al., 2014). The levels of HMGB1 in the blood are increased in patients with decreased cognition after gastrointestinal surgery (Lin et al., 2014). Since HMGB1 can bind TLR2 (Bae, 2012; Park et al., 2004), it is conceivable that HMGB1 is an upstream molecule for surgery to induce inflammation and cognitive dysfunction. Our results showed that surgery increased HMGB1 expression. Glycyrrhizin, a natural triterpene glycoside and a HMGB1 antagonist (Chen et al., 2017; Kim et al., 2012), attenuated the increase of HMGB1 in the nuclear fraction of cells, proinflammatory cytokine production in the brain tissues and dysfunction of learning and memory after surgery. These results support the role of HMGB1 in surgery-induced neuroinflammation and dysfunction of learning and memory. More importantly, glycyrrhizin blocked surgery-induced increase of total TLR2 protein and its membrane fraction, a functional site for TLRs. These results suggest that HMGB1 regulates the expression of TLR2. Since the increased HMGB1 at 6 h after surgery was mostly in the nuclear fraction, it is possible that HMGB1 may directly regulate the expression of TLR2. In addition to being secreted to extracellular space as an inflammatory mediator (Wang et al., 2014; Wang et al., 2004), HMGB1 can bind and bend DNA to facilitate the binding of transcription factors to the DNA. This HMGB1 binding may be more DNA local structure-dependent than specific

DNA sequence-dependent. For example, HMGB1 preferentially binds DNA containing cruciforms or bent structure (Stros, 2010). HMGB1 also interacts with nucleosomes to loosen packed DNA. These effects facilitate the transcription of corresponding gene(s) (Klune et al., 2008). Consistent with this possible mechanism, surgery increased the binding between HMGB1 and *tlr2* gene. Thus, our results provide initial evidence that HMGB1 increased TLR2 expression, a novel mechanism for surgery to increase TLR signaling. Our results also showed that TLR2 increase was mostly in the plasma membrane fraction. The increase was abolished by glycyrrhizin. These results suggest a role of HMGB1 in this TLR2 subcellular distribution. However, it is not known whether this distribution effect on TLR2 is related to the fact that TLR2 is a receptor for HMGB1 (Aucott et al., 2018; Bae, 2012; Park et al., 2004; Yu et al., 2006).

Based on the above discussion, our results suggest novel mechanisms for the development of POCD. First, surgery induces HMGB1 expression, which upregulates TLR2. Extracellular HMGB1 can bind TLR2 (Aucott et al., 2018; Bae, 2012; Park et al., 2004). These effects on TLR2 activate inflammatory process that leads to POCD. Thus, interventions to disrupt the interaction between HMGB1 and TLRs may be potential strategies to reduce POCD.

Many surgery models have been developed to study POCD in rodents. These models include abdominal surgery and orthopedic surgery (Chen et al., 2019; Cibelli et al., 2010) . We have been using a carotid artery exposure mode (Zhang et al., 2014b; Zheng et al., 2017). The advantage of our model may include less disturbance on digestive system (vs. abdominal surgery) and motor function (vs. orthopedic surgery). Disturbance on the digestive system may affect general health and normal motor functions are needed for the tasks of learning and memory.

Our study has limitations. Our data suggest that HMGB1 is a molecule upstream of TLR2 to mediate surgery-induced neuroinflammation and dysfunction of learning and memory. It is not known how surgery activates HMGB1. We have not determined whether HMGB1 regulates the expression of other TLRs. Also, TLR3 and TLR4 have been implied to play a role in the development of POCD (Chen et al., 2019; Wang et al., 2013). Our current study has shown that TLR2 contributes to POCD. The relative contribution of TLR2, TLR3 and TLR4 to the development of POCD is not clear and has not been determined in this study. One possibility is that these three TLRs or additional TLRs may interact to facilitate the inflammatory responses and ultimately lead to neuroinflammation and cognitive dysfunction. Finally, only male mice were used in the study to avoid the influence of menstrual cycle in learning and memory functions. Future studies will be performed to determine whether the findings from this study are applicable to female mice.

5. Conclusions

Our results suggest that TLR2 contributes to surgery-induced neuroinflammation and impairment of learning and memory. HMGB1 upregulates TLR2 expression after surgery to facilitate this contribution. Thus, TLR2 and HMGB1 are potential molecular targets for reducing POCD.

Funding:

Availability of data and materials:

Data will be available upon request.

Abbreviations

DMSO	dimethyl sulfoxide
GFAP	glial fibrillary acidic protein
HMGBl	high mobility group box-l
Iba-1	ionized calcium binding adapter molecule 1
IL	interleukin
NeuN	neuronal nuclei
NS	normal saline
NeuN	neuronal nuclei
POCD	postoperative cognitive dysfunction
RRID	research resource identifier
TBS	Tris-buffered saline
TLR2$^{-/-}$	TLR2 knockout
TLR	Toll-like receptor

References

Aucott H, Sowinska A, Harris HE & Lundback P, (2018). Ligation of free HMGB1 to TLR2 in the absence of ligand is negatively regulated by the C-terminal tail domain. Molecular Medicine, 24, 19. [PubMed: 30134807]

Bae JS, (2012). Role of high mobility group box 1 in inflammatory disease: focus on sepsis. Archives of Pharmacal Research, 35, 1511–1523. [PubMed: 23054707]

Bedford PD, (1955). Adverse cerebral effects of anaesthesia on old people. Lancet, 269, 259–263. [PubMed: 13243706]

Bi J, Shan W, Luo A & Zuo Z, (2017). Critical role of matrix metallopeptidase 9 in postoperative cognitive dysfunction and age-dependent cognitive decline. Oncotarget, 8, 51817–51829. [PubMed: 28881691]

Cao L, Li L, Lin D & Zuo Z, (2012). Isoflurane induces learning impairment that is mediated by interleukin 1beta in rodents. PLoS ONE, 7, e51431. [PubMed: 23251531]

Chen C, Gao R, Li M, Wang Q, Chen H, Zhang S, … Liu J, (2019). Extracellular RNAs-TLR3 signaling contributes to cognitive decline in a mouse model of postoperative cognitive dysfunction. Brain Behavior and Immunity, 80, 439–451.

Chen D, Bellussi LM, Cocca S, Wang J, Passali GC, Hao X, … Passali D, (2017). Glycyrrhetinic acid suppressed hmgb1 release by up-regulation of Sirt6 in nasal inflammation. Journal of Biological Regulators and Homeostatic Agents, 31, 269–277. [PubMed: 28685526]

Cheng K, Wang X, Zhang S & Yin H, (2012). Discovery of small-molecule inhibitors of the TLR1/TLR2 complex. Angewandte Chemie (International ed. in English), 51, 12246–12249. [PubMed: 22969053]

Cibelli M, Fidalgo AR, Terrando N, Ma D, Monaco C, Feldmann M, … Maze M, (2010). Role of interleukin-1beta in postoperative cognitive dysfunction. Annals of Neurology, 68, 360–368. [PubMed: 20818791]

d'Avila JC, Siqueira LD, Mazeraud A, Azevedo EP, Foguel D, Castro-Faria-Neto HC, … Bozza FA, (2018). Age-related cognitive impairment is associated with long-term neuroinflammation and oxidative stress in a mouse model of episodic systemic inflammation. Journal of Neuroinflammation, 15, 28. [PubMed: 29382344]

Faraco G, Fossati S, Bianchi ME, Patrone M, Pedrazzi M, Sparatore B, … Chiarugi A, (2007). High mobility group box 1 protein is released by neural cells upon different stresses and worsens ischemic neurodegeneration in vitro and in vivo. Journal of Neurochemistry, 103, 590–603. [PubMed: 17666052]

Feng C, Zhang Y, Yin J, Li J, Abounader R & Zuo Z, (2014). Regulatory factor X1 is a new tumor suppressive transcription factor that acts via direct downregulation of CD44 in glioblastoma. Neuro-oncology, 16, 1078–1085. [PubMed: 24526308]

Feng PP, Deng P, Liu LH, Ai Q, Yin J, Liu Z & Wang GM, (2017). Electroacupuncture Alleviates Postoperative Cognitive Dysfunction in Aged Rats by Inhibiting Hippocampal Neuroinflammation Activated via Microglia/TLRs Pathway. Evidence-based Complementary Alternative Medicine: eCAM, 2017, 6421260. [PubMed: 28684969]

Festoff BW, Sajja RK, van Dreden P & Cucullo L, (2016). HMGB1 and thrombin mediate the blood-brain barrier dysfunction acting as biomarkers of neuroinflammation and progression to neurodegeneration in Alzheimer's disease. Journal of Neuroinflammation, 13, 194. [PubMed: 27553758]

Ji YR, Kim HJ, Bae KB, Lee S, Kim MO & Ryoo ZY, (2015). Hepatic serum amyloid A1 aggravates T cell-mediated hepatitis by inducing chemokines via Toll-like receptor 2 in mice. The Journal of Biological Chemistry, 290, 12804–12811. [PubMed: 25847238]

Kawai T & Akira S, (2006). TLR signaling. Cell Death and Differentiation, 13, 816–825. [PubMed: 16410796]

Kawai T & Akira S, (2010). The role of pattern-recognition receptors in innate immunity: update on Toll-like receptors. Nature Immunology, 11, 373–384. [PubMed: 20404851]

Kilic U, Kilic E, Matter CM, Bassetti CL & Hermann DM, (2008). TLR-4 deficiency protects against focal cerebral ischemia and axotomy-induced neurodegeneration. Neurobiology of Disease, 31, 33–40. [PubMed: 18486483]

Kim SW, Jin Y, Shin JH, Kim ID, Lee HK, Park S, … Lee JK, (2012). Glycyrrhizic acid affords robust neuroprotection in the postischemic brain via anti-inflammatory effect by inhibiting HMGB1 phosphorylation and secretion. Neurobiology of Disease, 46, 147–156. [PubMed: 22266336]

Kim YM, Kim HJ & Chang KC, (2015). Glycyrrhizin reduces HMGB1 secretion in lipopolysaccharide-activated RAW 264.7 cells and endotoxemic mice by p38/Nrf2-dependent induction of HO-1. International Immunopharmacology, 26, 112–118. [PubMed: 25812767]

Klune JR, Dhupar R, Cardinal J, Billiar TR & Tsung A, (2008). HMGB1: endogenous danger signaling. Molecular Medicine (Cambridge, Mass.), 14, 476–484.

Kong ZH, Chen X, Hua HP, Liang L & Liu LJ, (2017). The Oral Pretreatment of glycyrrhizin prevents surgery-induced cognitive impairment in aged mice by reducing neuroinflammation and alzheimer's-related pathology via HMGB1 inhibition. Journal of Molecular Neuroscience: MN, 63, 385–395. [PubMed: 29034441]

Lehnardt S, Lehmann S, Kaul D, Tschimmel K, Hoffmann O, Cho S, … Weber JR, (2007). Toll-like receptor 2 mediates CNS injury in focal cerebral ischemia. Journal of Neuroimmunology, 190, 28–33. [PubMed: 17854911]

Li L, Deng J & Zuo Z, (2013). Glutamate transporter type 3 mediates isoflurane preconditioning-induced acute phase of neuroprotection in mice. Brain Research Bulletin, 98, 23–29. [PubMed: 23827345]

Lin F, Zheng Y, Pan L & Zuo Z, (2020). Attenuation of noisy environment-induced neuroinflammation and dysfunction of learning and memory by minocycline during perioperative period in mice. Brain Research Bulletin, 159, 16–24. [PubMed: 32208177]

Lin GX, Wang T, Chen MH, Hu ZH & Ouyang W, (2014). Serum high-mobility group box 1 protein correlates with cognitive decline after gastrointestinal surgery. Acta Anaesthesiologica Scandinavica, 58, 668–674. [PubMed: 24754551]

Lin Q, Li M, Fang D, Fang J & Su SB, (2011). The essential roles of Toll-like receptor signaling pathways in sterile inflammatory diseases. International Immunopharmacology, 11, 1422–1432. [PubMed: 21600309]

Lotze MT & Tracey KJ, (2005). High-mobility group box 1 protein (HMGB1): nuclear weapon in the immune arsenal. Nature Reviews. Immunology, 5, 331–342.

Lu SM, Gui B, Dong HQ, Zhang X, Zhang SS, Hu LQ, … Qian YN, (2015a). Prophylactic lithium alleviates splenectomy-induced cognitive dysfunction possibly by inhibiting hippocampal TLR4 activation in aged rats. Brain Research Bulletin, 114, 31–41. [PubMed: 25839444]

Lu SM, Yu CJ, Liu YH, Dong HQ, Zhang X, Zhang SS, … Gui B, (2015b). S100A8 contributes to postoperative cognitive dysfunction in mice undergoing tibial fracture surgery by activating the TLR4/MyD88 pathway. Brain, Behavior, and Immunity, 44, 221–234.

McKim DB, Niraula A, Tarr AJ, Wohleb ES, Sheridan JF & Godbout JP, (2016). Neuroinflammatory Dynamics Underlie Memory Impairments after Repeated Social Defeat. Journal of Neuroscience, 36, 2590–2604. [PubMed: 26937001]

Miyake K, (2007). Innate immune sensing of pathogens and danger signals by cell surface Toll-like receptors. Seminars in Immunology, 19, 3–10. [PubMed: 17275324]

Moller JT, Cluitmans P, Rasmussen LS, Houx P, Rasmussen H, Canet J, … Gravenstein JS, (1998). Long-term postoperative cognitive dysfunction in the elderly ISPOCD1 study. ISPOCD investigators. International Study of Post-Operative Cognitive Dysfunction. Lancet, 351, 857–861. [PubMed: 9525362]

Monk TG, Weldon BC, Garvan CW, Dede DE, van der Aa MT, Heilman KM & Gravenstein JS, (2008). Predictors of cognitive dysfunction after major noncardiac surgery. Anesthesiology, 108, 18–30. [PubMed: 18156878]

Muscat SM, Deems NP, D'Angelo H, Kitt MM, Grace PM, Andersen ND, … Barrientos RM, (2021). Postoperative cognitive dysfunction is made persistent with morphine treatment in aged rats. Neurobiology of Aging, 98, 214–224. [PubMed: 33341652]

Park JS, Svetkauskaite D, He Q, Kim JY, Strassheim D, Ishizaka A & Abraham E, (2004). Involvement of toll-like receptors 2 and 4 in cellular activation by high mobility group box 1 protein. The Journal of Biological Chemistry, 279, 7370–7377. [PubMed: 14660645]

Scaffidi P, Misteli T & Bianchi ME, (2002). Release of chromatin protein HMGB1 by necrotic cells triggers inflammation. Nature, 418, 191–195. [PubMed: 12110890]

Steinmetz J, Christensen KB, Lund T, Lohse N & Rasmussen LS, (2009). Long-term consequences of postoperative cognitive dysfunction. Anesthesiology, 110, 548–555. [PubMed: 19225398]

Stros M, (2010). HMGB proteins: interactions with DNA and chromatin. Biochimica et Biophysica Acta, 1799, 101–113. [PubMed: 20123072]

Terrando N, Brzezinski M, Degos V, Eriksson LI, Kramer JH, Leung JM, … Maze M, (2011). Perioperative cognitive decline in the aging population. Mayo Clinic Proceedings, 86, 885–893. [PubMed: 21878601]

Terrando N, Yang T, Wang X, Fang J, Cao M, Andersson U, … Tong J, (2016). Systemic HMGB1 neutralization prevents postoperative neurocognitive dysfunction in aged rats. Frontiers in Immunology, 7, 441. [PubMed: 27822212]

Vacas S, Degos V, Tracey KJ & Maze M, (2014). High-mobility group box 1 protein initiates postoperative cognitive decline by engaging bone marrow-derived macrophages. Anesthesiology, 120, 1160–1167.10.1097/ALN.0000000000000045 [PubMed: 24162463]

Wang H, Ward MF & Sama AE, (2014). Targeting HMGB1 in the treatment of sepsis. Expert Opinion on Therapeutic Targets, 18, 257–268. [PubMed: 24392842]

Wang H, Yang H & Tracey KJ, (2004). Extracellular role of HMGB1 in inflammation and sepsis. Journal of Internal Medicine, 255, 320–331. [PubMed: 14871456]

Wang Y, He H, Li D, Zhu W, Duan K, Le Y, … Ou Y, (2013). The role of the TLR4 signaling pathway in cognitive deficits following surgery in aged rats. Molecular Medicine Reports, 7, 1137–1142. [PubMed: 23426570]

Xing W, Huang P, Lu Y, Zeng W & Zuo Z, (2018). Amantadine attenuates sepsis-induced cognitive dysfunction possibly not through inhibiting toll-like receptor 2. Journal of Molecular Medicine (Berl), 96, 391–402.

Yang C, Sun S, Zhang Q, Guo J, Wu T, Liu Y, … Peng Y, (2020). Exosomes of Antler Mesenchymal Stem Cells Improve Postoperative Cognitive Dysfunction in Cardiopulmonary Bypass Rats through Inhibiting the TLR2/TLR4 Signaling Pathway. Stem Cells International, 2020, 2134565. [PubMed: 32300366]

Yu M, Wang H, Ding A, Golenbock DT, Latz E, Czura CJ, … Yang H, (2006). HMGB1 signals through toll-like receptor (TLR) 4 and TLR2. Shock, 26, 174–179. [PubMed: 16878026]

Zeng Q, Shan W, Zhang H, Yang J & Zuo Z, (2021). Paraventricular thalamic nucleus plays a critical role in consolation and anxious behaviors of familiar observers exposed to surgery mice. Theranostics, 11, 3813–3829. [PubMed: 33664863]

Zhang J, Jiang W & Zuo Z, (2014a). Pyrrolidine dithiocarbamate attenuates surgery-induced neuroinflammation and cognitive dysfunction possibly via inhibition of nuclear factor kappaB. Neuroscience, 261, 1–10. [PubMed: 24365462]

Zhang J, Tan H, Jiang W & Zuo Z, (2014b). Amantadine alleviates postoperative cognitive dysfunction possibly by increasing glial cell line-derived neurotrophic factor in rats. Anesthesiology, 121, 773–785. [PubMed: 25251457]

Zheng B, Lai R, Li J & Zuo Z, (2017). Critical role of P2X7 receptors in the neuroinflammation and cognitive dysfunction after surgery. Brain, Behavior, and Immunity, 61, 365–374.

Ziegler G, Harhausen D, Schepers C, Hoffmann O, Rohr C, Prinz V, … Trendelenburg G, (2007). TLR2 has a detrimental role in mouse transient focal cerebral ischemia. Biochemical and Biophysical Research Communications, 359, 574–579. [PubMed: 17548055]
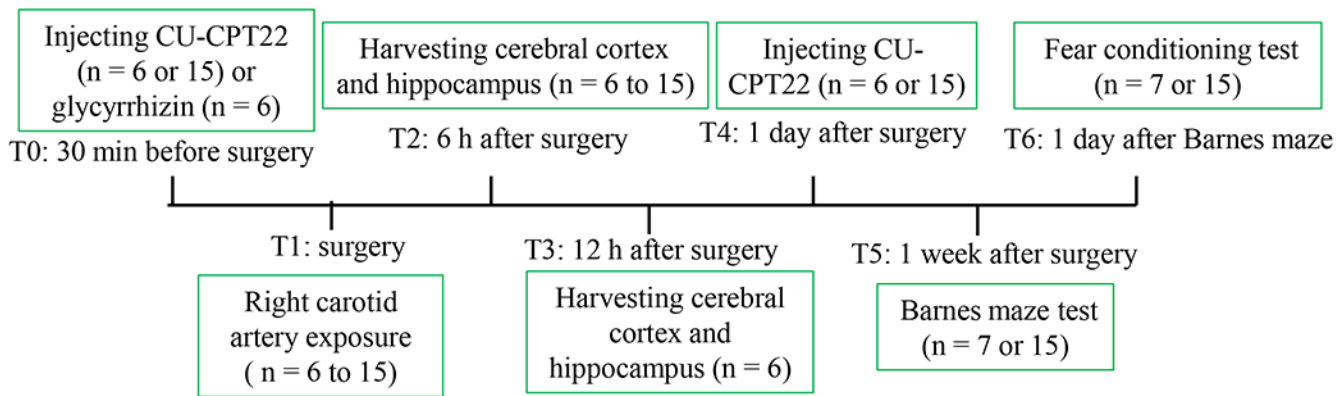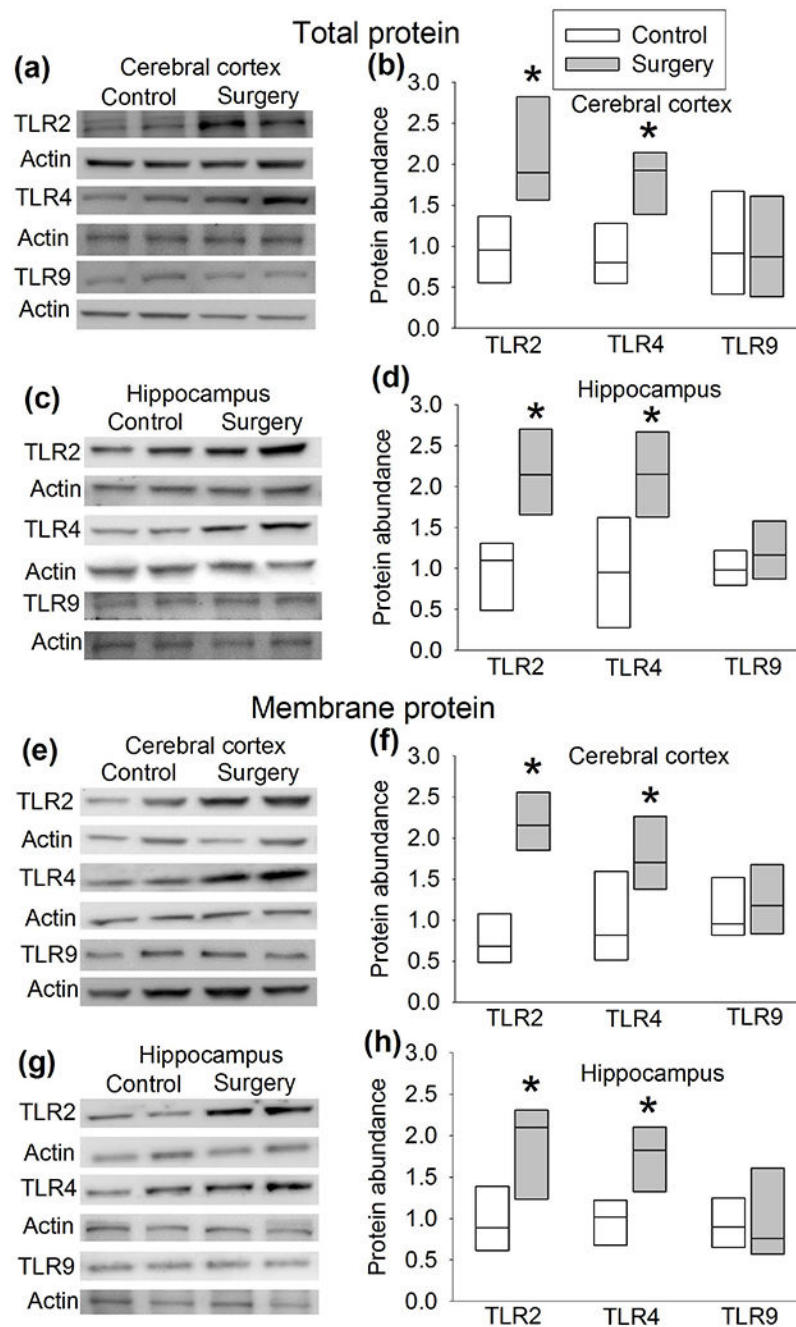
Figure 1.
Diagram of time-line of experimental procedures. Procedures at 7 time points (T0 to T6) are described (the n number in the diagram referred to the number of animals per group).

Figure 2.
Surgery increased the expression of TLR2 and TLR4. CD-1 mice were subjected to right carotid artery exposure under isoflurane anesthesia. Cerebral cortex and hippocampus were harvested 6 h after the surgery. (a) Representative Western blotting images of total protein from the cerebral cortex. (b) Quantitative results of total TLR2, TLR4 and TLR9 protein abundance from the cerebral cortex. (c) Representative Western blotting images of total protein from the hippocampus. (d) Quantitative results of total TLR2, TLR4 and TLR9 abundance from the hippocampus. (e) Representative Western blotting images of membrane

protein from the cerebral cortex. (f) Quantitative results of membrane TLR2, TLR4 and TLR9 abundance from the cerebral cortex. (g) Representative Western blotting images of membrane protein from the hippocampus. (h) Quantitative results of membrane TLR2, TLR4 and TLR9 abundance from the hippocampus. Results are in box plot format (n = 6, the n number referred to the number of animals). ● : lowest or highest score (the score will not show up if it falls in the 95th percentile); between lines: 95th percentile of the data; inside boxes: 25th to 75th percentile including the median of the data. * $P < 0.05$ compared with control.
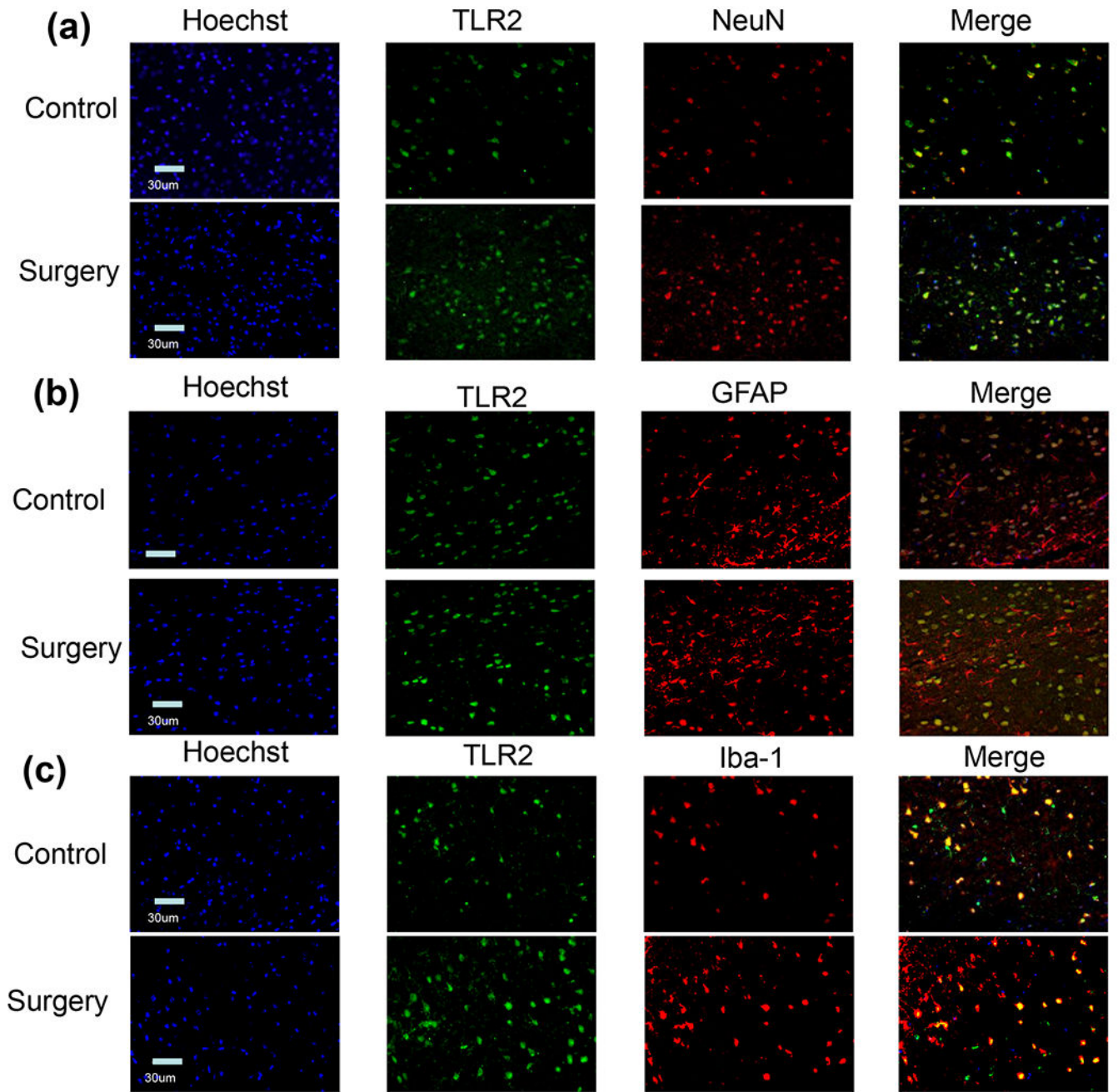
Figure 3.
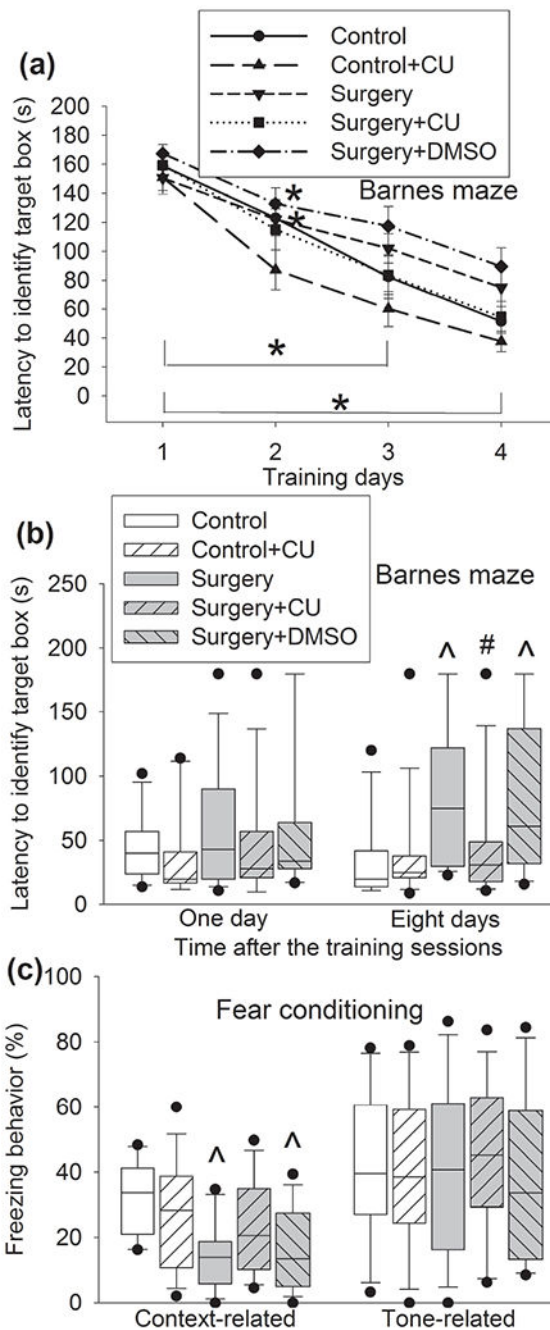Immunofluorescence staining of TLR2 and various cell-type markers. Scale bar = 30 μm.

Figure 4.
CU-CPT22 attenuated surgery-induced learning and memory dysfunction in CD-1 mice.
Mice were subjected to Barnes maze and fear conditioning tests from 1 week after surgery.
(a) Training sessions of Barnes maze test. (b) Memory phase of Barnes maze test. The
results of memory phase were not normally distributed (P < 0.05 by Kolmogorov-Smirnov
test for normality). (c) Fear conditioning test. Results in panel a are means ± S.E.M. (n =
15, the n number referred to the number of animals). Results in other panels are in box plot
format (n = 15, the n number referred to the number of animals). ● : lowest or highest score

(the score will not show up if it falls in the 95th percentile); between lines: 95th percentile of the data; inside boxes: 25th to 75th percentile including the median of the data. * $P < 0.05$ compared with the corresponding data on day 1. ^ $P < 0.05$ compared with control. # $P < 0.05$ compared with surgery alone. CU: CU-CPT22.
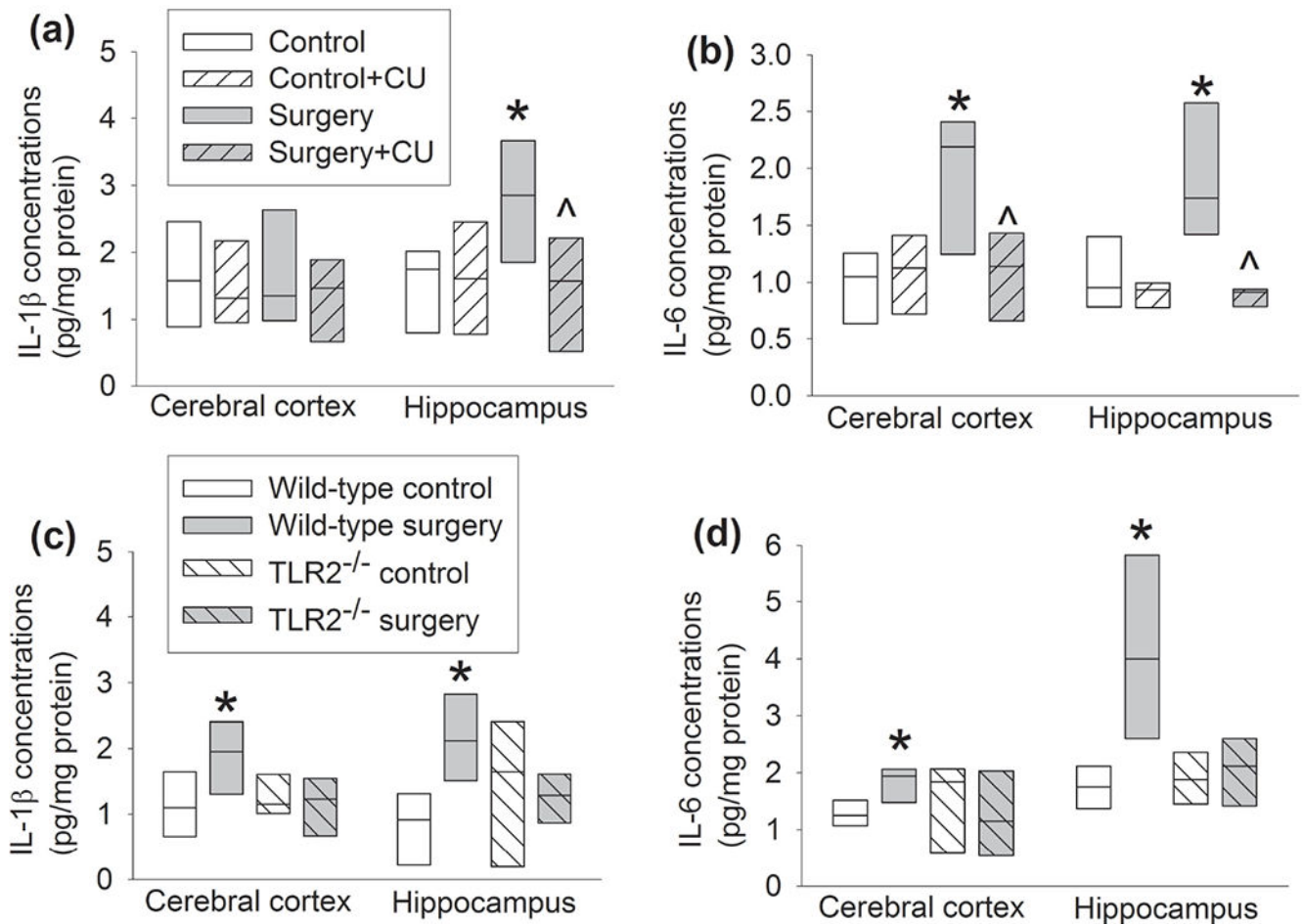
Figure 5.
Surgery increased proinflammatory cytokines in the hippocampus and cortex of mice. Hippocampus and cerebral cortex were harvested 12 h after surgery. (a) IL-1β levels in CD-1 mice. (b) IL-6 levels in CD-1 mice. (c) IL-1β levels in C57BL/6J and TLR2$^{-/-}$ mice. (d) IL-6 levels in C57BL/6J and TLR2$^{-/-}$ mice. Results are in box plot format (n = 6, the n number referred to the number of animals). ● : lowest or highest score (the score will not show up if it falls in the 95th percentile); between lines: 95th percentile of the data; inside boxes: 25th to 75th percentile including the median of the data. * $P < 0.05$ compared with control alone. ^ $P < 0.05$ compared with surgery alone.
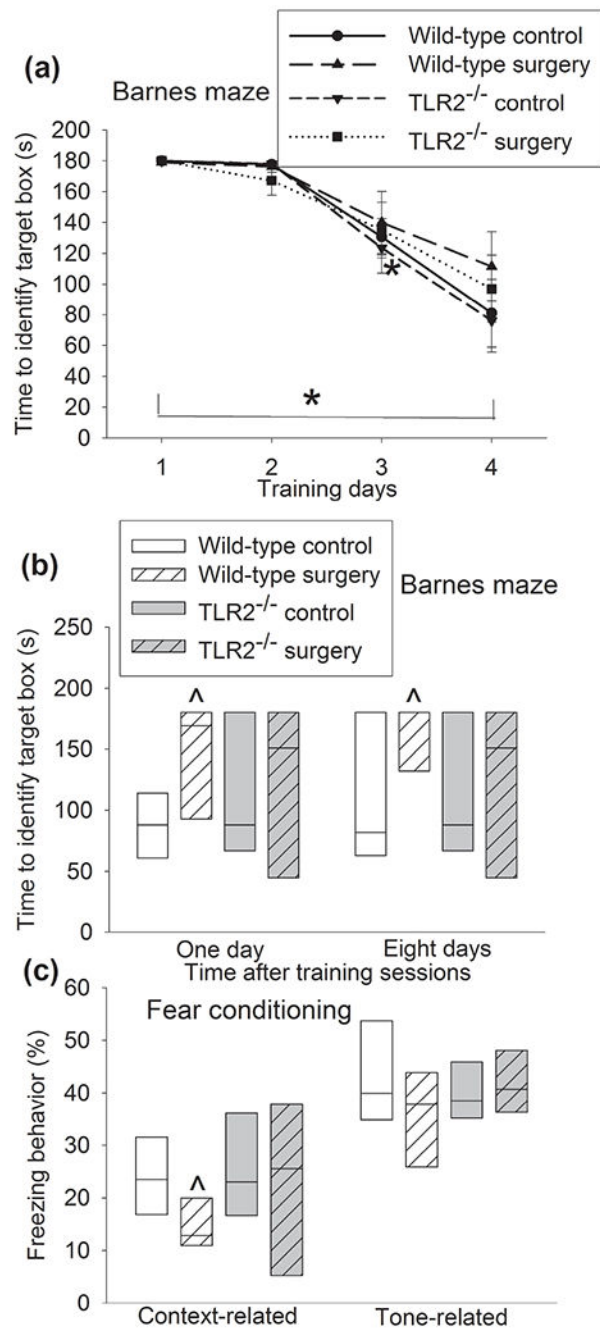
Figure 6.
TLR2 knockout attenuated surgery-induced learning and memory dysfunction in mice.
C57BL/6J mice and TLR2$^{-/-}$ mice were subjected to Barnes maze and fear conditioning
tests from 1 week after surgery. (a) Training sessions of Barnes maze test. (b) Memory phase
of Barnes maze test. (c) Fear conditioning tests. Results in panel a are means ± S.E.M. (n =
7, the n number referred to the number of animals). Results in other panels are in box plot
format (n = 7, the n number referred to the number of animals). ● : lowest or highest score
(the score will not show up if it falls in the 95th percentile); between lines: 95th percentile of

the data; inside boxes: 25th to 75th percentile including the median of the data. * $P < 0.05$ compared with the corresponding data on day 1. ^ $P < 0.05$ compared with control.
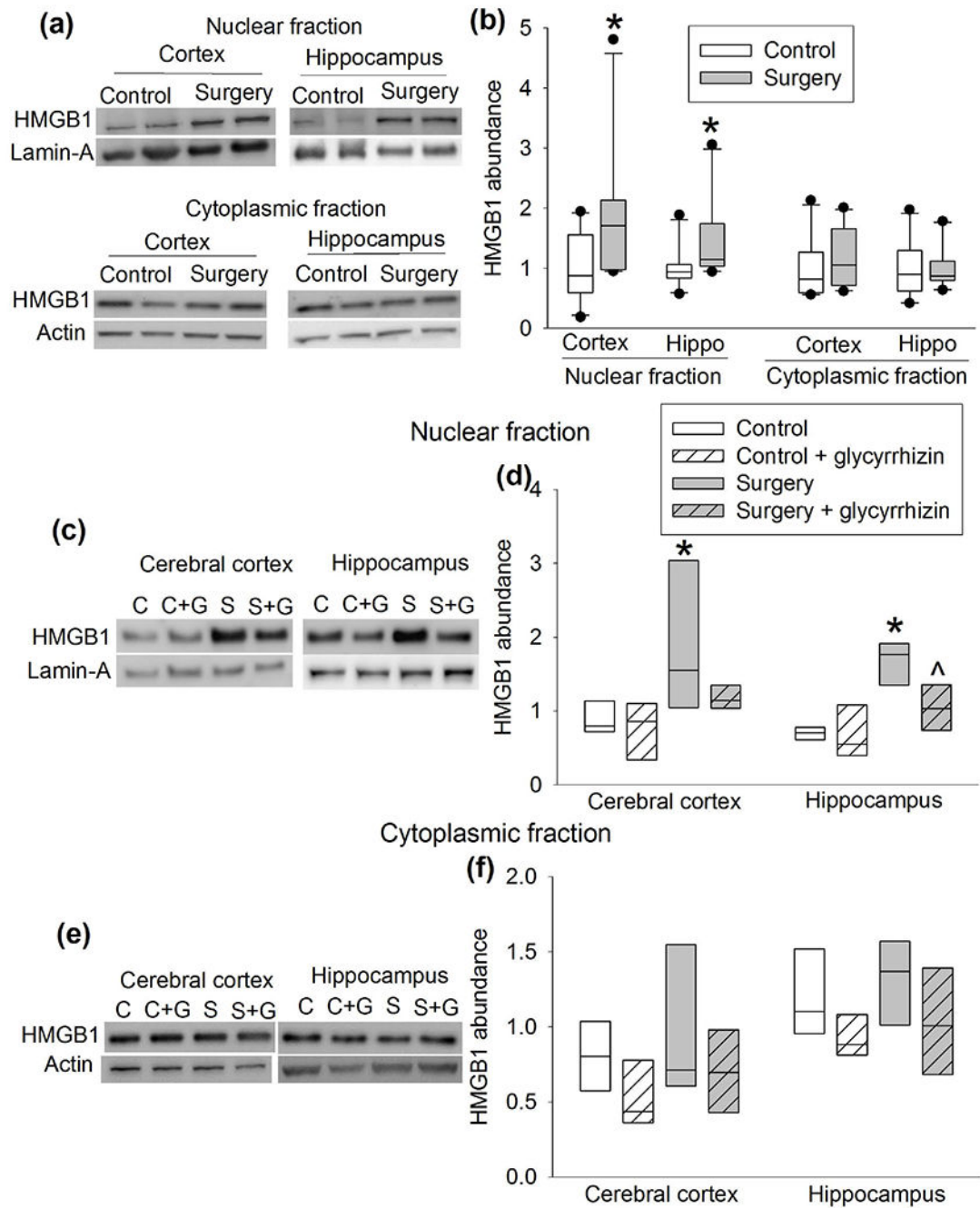
Figure 7.

Surgery increased HMGB1 expression. CD-1 mice were subjected to right carotid artery exposure under isoflurane anesthesia. Cerebral cortex and hippocampus were harvested 6 h after the surgery. (a) Representative Western blotting images of samples from mice with or without surgery. (b) Quantitative results of HMGB1 protein abundance in samples from mice with or without surgery. (c) Representative Western blotting images of nuclear proteins from mice with or without surgery in the presence or absence of glycyrrhizin. (d) Quantitative results of HMGB1 protein abundance in nuclear proteins from mice

with or without surgery in the presence or absence of glycyrrhizin. (e) Representative Western blotting images of cytoplasmic proteins from mice with or without surgery in the presence or absence of glycyrrhizin. (f) Quantitative results of HMGB1 protein abundance in cytoplasmic proteins from mice with or without surgery in the presence or absence of glycyrrhizin. Results are in box plot format (n = 10 for panel b, = 6 for panels d and f; the n number referred to the number of animals). ● : lowest or highest score (the score will not show up if it falls in the 95th percentile); between lines: 95th percentile of the data; inside boxes: 25th to 75th percentile including the median of the data. * $P < 0.05$ compared with control. ^ $P < 0.05$ compared with surgery alone.
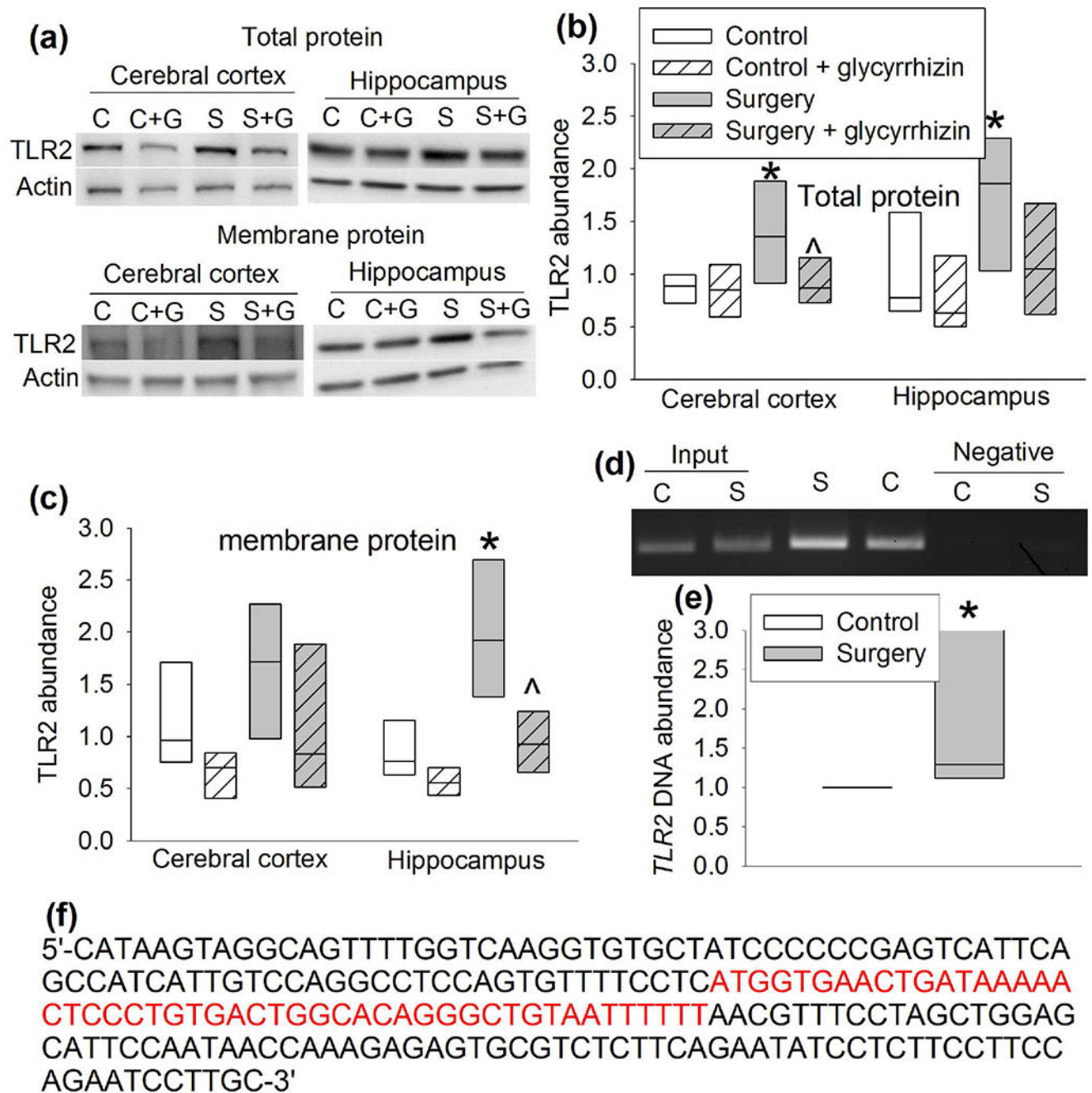
Figure 8.
HMGB1 regulated TLR2 expression. CD-1 mice were subjected to right carotid artery exposure under isoflurane anesthesia and treated with or without glycyrrhizin. Cerebral cortex and hippocampus were harvested 6 h after the surgery. (a) Representative Western blotting images of total or membrane protein. (b) Quantitative results of TLR2 abundance in total protein. (c) Quantitative results of TLR2 abundance in membrane protein. (d) Representative images of the PCR products of *tlr2* gene fragment (−283 bp to −71 bp). The first two lanes are input controls and the last two lanes are negative IgG controls.

(e) Quantitative results of the PCR products of *tlr2* gene fragment (−283 bp to −71 bp). These PCR results were not normally distributed (P < 0.05 by Kolmogorov-Smirnov test for normality). (f) The sequence of the segment of the *tlr2* gene that was immunoprecipitated by an anti-HGMB1 antibody. The presumed binding sequence for HGMB1 is in red. Results are in box plot format (n = 6 for panels b and c, = 15 for panel e; the n number referred to the number of animals). ● : lowest or highest score (the score will not show up if it falls in the 95th percentile); between lines: 95th percentile of the data; inside boxes: 25th to 75th percentile including the median of the data. * $P < 0.05$ compared with control. ^ $P < 0.05$ compared with surgery alone. C: control, S: surgery.